Electronic Structure and Conformational Conversion of Calix[4]arene Complexes with Alkali Metal Ions

Yoshiya Inokuchi,* Kenta Hirai, and Takayuki Ebata

Department of Chemistry, Graduate School of Science, Hiroshima University, Higashi-Hiroshima, Hiroshima 739-8526, Japan

E-mail: y-inokuchi@hiroshima-u.ac.jp

Phone: +81 (Japan)-82-424-7101

Abstract

Ultraviolet photodissociation (UVPD) spectra of calix[4]arene (C4A) complexes with alkali metal ions, M^+•C4A (M = Na, K, Rb, and Cs), are measured in the 34000–37000 cm^{-1} region under cold (~10 K) conditions in the gas phase. The Na^+•C4A and K^+•C4A complexes show several sharp vibronic bands, while the UVPD spectra of the Rb^+•C4A and Cs^+•C4A complexes exhibit only broad features. The UVPD spectra are assigned with the aid of quantum chemical calculations. Most of the features in the UVPD spectra can be attributed to cone isomers, which are the most stable for all the M^+•C4A complexes. In all the cone isomers, the M^+ ion is encapsulated inside the cavity of C4A, and the structure is distorted to C_2 symmetry from that of bare C4A (C_4 symmetry). The cone isomers show a big difference in the electronic structure between the K^+ and Rb^+ complexes. The Rb^+ and Cs^+ complexes have an electronic structure similar to that of bare C4A. In the Na^+ and K^+ complexes, a pair of two benzene rings facing to each other has a short distance between them (< 6

Å). This results in substantial overlap of π clouds between them, and an electronic transition is localized on this pair. Only this localized electronic transition of the Na^+ and K^+ complexes shows sharp band features in the UVPD spectra. In the Na^+•C4A complex, the UVPD spectroscopic result suggests the coexistence of other isomers having a partial cone and 1,3-alternate form. The energetics for isomerization reactions of C4A and Na^+•C4A is examined theoretically. Estimated potential barriers between the stable conformers are less than 75 kJ/mol for Na^+•C4A, suggesting that conformational conversion can occur at room temperature, before the Na^+•C4A complex enters the cold ion trap. The existence of multiple conformations for Na^+•C4A is attributed to higher stability of these conformers, both kinetically and thermodynamically, compared to the case of bare C4A and the other M^+•C4A complexes.

*To whom correspondence should be addressed.

1. Introduction

Calixarenes (CAs) have been extensively utilized as host molecules in supramolecular chemistry.[1-11] Calix[4]arene (C4A, Scheme 1) is the smallest CA, and its derivatives can encapsulate guest species selectively, which can be controlled by the introduction of functional groups and the conformation.[6, 8, 12, 13] For C4A derivatives, there are four stable conformations: cone, partial-cone, 1,2-alternate, and 1,3-alternate.[3, 6, 14] The conformation and free energies for the conformational interconversion were determined in solution by temperature-dependent ^{1}H NMR spectroscopy;[14, 15] *p*-alkyl-C4As prefer to have cone conformations, but the inversion of the cone also occurs at room temperature.[14] Free energies of activation for the conformational inversion of C4A derivatives in solution were estimated as ~14 kcal/mol (~57 kJ/mol).[14] X-ray diffraction studies also suggested cone conformations for C4A derivatives in the solid state.[16, 17] The preference of the cone conformation in C4A is due to strong hydrogen-bonding interactions between the four OH groups.[3, 14] Metal ion–CA complexes were extensively studied as simple systems with charged guests. Izatt and co-workers reported cation transport by CA derivatives from alkali cation mixtures in solution, and the greatest selectivity of Cs^+ over Rb^+, K^+, and Na^+ was found with *p*-alkyl-C4As.[12, 13] Klinowski and co-workers reported solid-state NMR studies of *p*-tert-butyl-C4A complexes with alkali metal ions.[18] *p*-tert-butyl-C4A forms complexes with Li^+ and Na^+ due to electrostatic interactions between the cation and the phenolic oxygen atoms. In contrast, Cs^+ ion is encapsulated inside the cone due to dispersion and induction interactions.[18] Bernardino and Cost Cabral reported similar structures in their theoretical study on C4A complexes with alkali metal ions.[19] Shinkai and co-workers synthesized a number of C4A derivatives and succeeded in controlling their conformations.[4-8] They demonstrated that the metal ion selectivity of

C4A derivatives is highly dependent on their conformations.[8] In addition, they showed an unambiguous ^{1}H NMR evidence for intramolecular metal-ion exchange (Ag^+, K^+, and Na^+) between two binding sites in 1,3-alternate conformers of C4A derivatives.[5]

As mentioned above, the conformation of the CA complexes was analyzed mainly with X-ray crystallographic analysis and NMR spectroscopy, but their electronic structure has not been understood very well. Since C4A has four benzene chromophores and they interact with each other, it will be quite interesting how the inclusion of guest species affects the electronic structure of C4A. Since UV spectra of C4A derivatives in solution at room temperature show only broad features,[20] it is difficult to extract the absorption of C4A complexes with guests selectively from them. Hence, spectroscopic techniques free from spectral broadening due to the solvent and temperature effect and from ambiguity of observed species are needed to examine the electronic structure of C4A complexes in detail. Recently, laser spectroscopic methods coupled with cooling techniques such as free jet expansion and cold ion traps have been applied to complexes of macromolecules in the gas phase. The structure of cold inclusion complexes of C4A with neutral guests was investigated under free jet conditions.[21-24] The experimental and theoretical results suggest that all the inclusion complexes of C4A preferentially adopt *endo* forms with cone conformations. For electronic spectroscopy of ionic complexes, UV photodissociation (UVPD) spectroscopy under cold conditions in the gas phase is a very powerful technique.[25-27] UVPD spectroscopy has been used for ion complexes of crown ethers to examine the geometric and electronic structures.[28-36]

In this study, we investigate the relation between the conformation and the electronic structure of alkali metal ion–C4A complexes, M^+•C4A (M = Na, K, Rb, and

Cs), by means of gas-phase laser spectroscopy. UVPD spectra of the M^+•C4A complexes are measured in the 34000–37000 cm^{-1} region under cold gas-phase conditions, and the conformation of the M^+•C4A complexes are determined with the UVPD results with the aid of quantum chemical calculations. Based on the conformation determined in this study, the electronic structure of the M^+•C4A complexes is discussed. In addition, the energetics of isomerization reactions of C4A and Na^+•C4A is examined on the basis of quantum chemical calculations to explain the existence of multiple conformations in the UVPD results and isomerization processes that were observed experimentally in solution.

2. Experimental and Computational Methods

Figure 1 shows a schematic drawing of an electrospray ion source/cold ion trap/mass spectrometer system used for UVPD spectroscopy in this study. Details of the experiment have been described in our previous papers.[35-37] Briefly, the M^+•C4A (M = Na, K, Rb, and Cs) complexes are produced by electrospraying methanol solutions of MCl salt and C4A (~100 μM each), and introduced into a cold, Paul-type quadrupole ion trap (QIT) through a vaporization tube and two octopole ion guides (OPIGs). The QIT is cooled to ~4 K by a He cryostat, and He buffer gas is continuously introduced into the QIT. Ions are stored in the QIT for ~90 ms and cooled translationally and internally by the collision with the cold He buffer gas. The vibrational temperature of trapped ions was estimated as ~10 K in our previous study.[37] Ions other than parent ions of interest can be removed from the QIT by an RF potential applied to the entrance end cap.[38] The M^+•C4A complexes are then irradiated by a tunable UV laser, and resulting fragment M^+ ions are mass-analyzed and detected with a home-made

time-of-flight mass spectrometer.[39] UVPD spectra are obtained by plotting yields of the fragment M^+ ions against the wavenumber of the UV laser. The UV light for the photodissociation is obtained from a nanosecond optical parametric oscillator (EKSPLA, NT342B) with a repetition rate of 10 Hz and a linewidth of < 8 cm^{-1}.

Quantum chemical calculations are also performed for the M^+•C4A complexes. The structure of the M^+•C4A complexes is optimized with the GAUSSIAN09 program package at the M05-2X/6-31+G(d) level of theory.[40, 41] The transition energy and the oscillator strength are obtained by time-dependent density functional theory (TD-DFT) calculations at the M05-2X/6-31+G(d) level. For comparison of calculated UV spectra with the UVPD results, a scaling factor of 0.8426 is employed for the calculated transition energy. This factor is determined so as to reproduce the position of a sharp UVPD band of the K^+•C4A complex at 36156 cm^{-1} with the S_2–S_0 transition energy of the most stable conformer.[37] For Rb and Cs, we use the Stuttgart RLC as effective core potentials (ECPs). Functions of the ECPs are obtained from a database of basis sets.[42, 43] The combination of the calculation level (M05-2X/6-31+G(d)) and the ECPs (Stuttgart RLC) has been applied to many ion complexes of benzo-crown ethers and has succeeded very well in predicting the geometric and electronic structures.[28-31, 35, 36] For C4A and Na^+•C4A, we obtain the structure and the energy of transition-state conformations between stable conformers (cone, partial-cone, 1,2-alternate, and 1,3-alternate) by using the GAUSSIAN09 program package with the Opt = QST3 keyword. We confirm the transition-state conformations by performing vibrational analysis and checking if there is one imaginary frequency correlating to two stable conformations.

3. Results and Discussion

3.1. UV Photodissociation Spectra

Figure 2 displays the UVPD spectra of the M^+•C4A (M = Na, K, Rb, and Cs) complexes in the 34000–37000 cm^{-1} region with the electronic spectrum of jet-cooled C4A.[21] The UVPD spectrum of the K^+•C4A complex in the 35800–36600 cm^{-1} region was already reported in our previous paper.[37] The K^+•C4A complex has a strong sharp band at 36156 cm^{-1}, accompanied with several sharp bands around it. The band at 36156 cm^{-1} was assigned to the band origin of the S_2–S_0 transition of the *endo* isomer.[37] Despite of the cooling of the ions in the QIT, the Rb^+•C4A and Cs^+•C4A complexes show only broad features in the UVPD spectra. In the spectrum of the Rb^+•C4A complex (Figure 2c), two absorption maxima are found around 36080 and 36380 cm^{-1}. For the Cs^+•C4A complex (Figure 2d), the absorption can be seen in the region of 35500–37000 cm^{-1} with two maxima at ~35920 and ~36360 cm^{-1}. The interval between the two maxima seems to be larger for the Cs^+ complex than that for the Rb^+ one. In the case of the Na^+ complex (Figure 2a), a resolved band is observed at 36202 cm^{-1} with a few sharp bands on the higher frequency side, similar to the case of the K^+•C4A complex. One big difference between the Na^+ and K^+ complexes is that there is very broad absorption in the 34000–36000 cm^{-1} region for the Na^+•C4A complex. Since a part of the UVPD spectrum of the Na^+•C4A complex shows resolved features, the broad nature of the absorption in the lower frequency region is not due to insufficient cooling of the ions. In the next section, we will determine the conformation and the electronic structure of the M^+•C4A complexes by using these UVPD results with the aid of quantum chemical calculations.

3.2. Geometric and Electronic Structures of the M^+•C4A Complexes

Figure 3 displays stable structures of the K^+•C4A complex and bare C4A having a cone form.[21] The structures of K^+•C4A in Figure 3 (KC4A-I, KC4A-II, and KC4A-III) have been found theoretically in our previous study.[37] Isomer KC4A-I (Figure 3a) has the K^+ ion in the cavity, having C_2 symmetry. In KC4A-II and KC4A-III (Figures 3b and 3c), the K^+ ion is located outside the cone, attached to one of the benzene rings or on the bottom. In addition to them, other three stable isomers (KC4A-IV, KC4A-V, and KC4A-VI) are found in this study (Figure 4). In these isomers, the C4A part has a partial-cone, 1,3-alternate, and 1,2-alternate conformation.[3, 6, 14] These types of C4A isomers were synthesized by Ikeda and Shinkai.[5] Also for the M^+•C4A (M = Na, Rb, and Cs) complexes, isomers similar to the forms of K^+•C4A in Figures 3 and 4 are found in our calculations. These isomers are called MC4A-I to MC4A-VI (M = Na, K, Rb, and Cs), and all the isomers of the M^+•C4A complexes are displayed in the Electronic Supplementary Information. Table 1 shows the total energy of the six isomers relative to that of MC4A-I. For all the M^+•C4A complexes, isomer MC4A-I is the most stable among the six forms. The second most stable isomer is MC4A-IV; the energy relative to that of the most stable one becomes smaller and smaller with decreasing the ion size from Cs^+ (25.1 kJ/mol) to Na^+ (11.2 kJ/mol). Based on the calculated total energy in Table 1, the UVPD spectra of the M^+•C4A complexes can be attributed mainly to isomers MC4A-I.

TD-DFT results of isomers MC4A-I reasonably explain overall features of the UVPD spectra. Figure 5 displays the results of the TD-DFT calculations for MC4A-I (red bars) with the UVPD spectra (black curves). Table 2 shows the calculated transition energy and oscillator strength of isomers MC4A-I. Isomers MC4A-I each

have four electronic states, S_1 to S_4, in this region. Among them, two states have large oscillator strengths for the transitions from the S_0 state. The UVPD spectra of the M^+•C4A complexes are assigned to the two strong transitions of MC4A-I, as shown with dotted lines in Figure 5. For the Na^+•C4A complex, the component starting from 36202 cm^{-1} and another one with a maximum at ~36780 cm^{-1} in the UVPD spectrum are attributed to the S_2–S_0 and S_4–S_0 transitions of NaC4A-I, respectively. Two components of the Rb^+•C4A complex at ~36080 and ~36380 cm^{-1} are assignable to the S_2–S_0 and S_3–S_0 transitions of RbC4A-I. In the case of the Cs^+•C4A complex, the broad bands at ~35920 and ~36360 cm^{-1} are ascribed to the S_2–S_0 and S_3–S_0 transitions of CsC4A-I. For the K^+•C4A complex, the S_3–S_0 transition of KC4A-I may provide the broad absorption around 36300 cm^{-1} in the UVPD spectrum, although a weak band at 36515 cm^{-1} was tentatively assigned to the origin band of the S_3–S_0 transition in our previous study.[37]

Figure 6 shows geometric parameters of MC4A-I (M = Na, K, Rb, and Cs) with those of C4A-I (Figure 3d). The definition of the geometric parameters (θ, d_1, and d_2) can be found in Figure 3a; θ is the plane angle of a benzene pair facing to each other, d_1 is the distance between the centers of the two benzene rings, and d_2 is the distance between the M^+ ion and the mean plane of the four oxygen atoms. Black lines in Figure 6 show the values of C4A-I. As seen in Figures 6a and 6b, the θ and d_1 values of the two benzene pairs in the Na^+ complex (NaC4A-I) are substantially different from each other. C4A-I has a cone-type, C_4 form; this originates from the strong hydrogen-bonding network formed with the four phenolic OH groups.[21] However, the inclusion of alkali metal ions in the cone of C4A highly distorts the cone. The θ and d_1 values then gradually approach those of bare C4A from Na^+ to Cs^+. The

distance between the M^+ ion and the oxygen plane (d_2, Figure 6c) becomes larger and larger with increasing the ion size. As mentioned above, C4A derivatives tend to capture Cs^+ ion preferentially in solution among alkali metal ions.[13] Hence, the preference of Cs^+ ion by C4A in solution can be ascribed to the least distorted form of the Cs^+•C4A complex, keeping the hydrogen-bonding network of the four OH groups.

As seen in Figure 5, the positions of the two strong electronic transitions calculated for MC4A-I (the red bars in Figure 5) do not show a monotonous trend against the ion size. The electronic transitions basically shift to higher frequencies from the Cs^+•C4A to Na^+•C4A complexes, but the interval of the two transitions becomes smaller from Cs^+ to K^+, and it becomes larger again from K^+ to Na^+. The origin of this trend can be found in molecular orbitals (MOs) that are involved in the electronic transitions of MC4A-I. Figure 7 displays the calculated energy of the electronic excited states, S_1 to S_4, for isomers MC4A-I and C4A-I. The energy levels of C4A-I are shown in the rightmost column of Figure 7. MOs that contribute the most to the electronic transitions of C4A-I and MC4A-I are shown in Figures 8 and 9, respectively. In Figure 7, the electronic states having large oscillator strengths from the S_0 state are drawn with red lines. For C4A-I (C_4 symmetry), the S_2 and S_3 states are degenerate, and the S_2–S_0 and S_3–S_0 transitions are mainly due to electron promotion from two degenerate MOs (HOMO–1 and HOMO–2) to the lowest unoccupied MO (LUMO), as seen in Figure 8. These electronic transitions of C4A partly have a charge-transfer nature from one pair of two benzene rings to the other, because the HOMO–1 and HOMO–2 orbitals are localized almost on one of the two benzene pairs, whereas the LUMO is delocalized equally on the four benzene rings. Attachment of M^+ ion breaks the symmetry from C_4 to C_2, and the S_2 and S_3 states are no longer degenerate as seen in CsC4A-I (Figure 7). However, as seen in Figure 9d, the features

of the MOs responsible for the electronic transitions of CsC4A-I are similar to those of C4A-I. A similar trend can be seen for the Rb^+ complex; the MOs relevant to the S_2–S_0 and S_3–S_0 transitions are quite similar between RbC4A-I and CsC4A-I (Figures 9c and 9d). However, a drastic change happens in the electronic structure between the Rb^+ and K^+ complexes in the series of alkali metal ions. The distance of one benzene pair in KC4A-I (5.76 Å, see Figure 6b) is shorter than that in RbC4A-I, and an unoccupied MO is formed with a localized nature on this pair, as seen in Figure 9b (LUMO+1). As a result, the S_2–S_0 transition of KC4A-I is highly localized on this pair. Based on the features of the MOs, the S_2–S_0 and S_3–S_0 transitions of RbC4A-I correspond to the S_3–S_0 and S_2–S_0 transitions of KC4A-I, respectively. For KC4A-I, the LUMO+1 can be stabilized by overlap of π MOs (Figure 9b). This results in a lower transition energy for the S_2–S_0 transition of KC4A-I, and the switching of the order of the electronic states occurs between RbC4A-I and KC4A-I as seen in Figure 7. This electronic interaction for KC4A-I is more obvious for NaC4A-I. The benzene distance of one pair is shorter (5.21 Å, Figure 6b) than that of KC4A-I, resulting in substantial overlap of π clouds between the two facing benzene rings in an unoccupied MO (LUMO, Figure 9a). As a result, the S_2 level becomes much more stabilized, providing a larger separation between the S_2 and S_3 states for the Na^+ complex than that for the K^+ complex. Comparison of the UVPD spectra with the TD-DFT results (Figure 5) suggests that only the localized electronic transition (S_2–S_0) of the Na^+ and K^+ complexes shows sharp band features in the UVPD spectra. As mentioned above, the strong electronic transitions of MC4A-I other than the S_2–S_0 transition of NaC4A-I and KC4A-I have a charge-transfer nature. This could be a reason for a big difference in the structure between the electronic ground and excited states, providing broad band features in the UVPD spectra.

Finally, we are left with the description of the broad absorption of the Na^+•C4A complex in the region lower than 36200 cm^{-1}. One plausible assignment of this feature is to the second and third most stable isomers, NaC4A-IV and NaC4A-V. The structures of these isomers are shown in Figure 10. Figure 5a also shows the TD-DFT results of NaC4A-IV and NaC4A-V (blue and black bars, respectively). Isomers NaC4A-IV and NaC4A-V have strong electronic transitions on the lower frequency side of the S_2–S_0 transition of NaC4A-I. This coincides with the UVPD spectral feature that broad absorption appears on the red side of the 36202-cm^{-1} band for Na^+•C4A (Figure 2a). In addition, these Na^+•C4A conformers (NaC4A-IV and NaC4A-V) have a smaller total energy (11.2 and 22.3 kJ/mol) than that of the other complexes (MC4A-IV and MC4A-V with M = K, Rb, and Cs, see Table 1). This also agrees with the UVPD result that additional absorption in the lower frequency region is highly enhanced only for the Na^+•C4A complex. The very broad features in the UVPD spectrum of the Na^+•C4A complex may probably reflect a fast dynamics due to a floppy nature of Na^+ encapsulation in the electronic excited states.

3.3. Energetics on Isomerization Reactions of C4A and M^+•C4A

As mentioned in the Introduction section, temperature-dependent NMR studies suggested that conformational inversion of cone-shaped C4A derivatives occurs in solution at room temperature.[14] Kämmerer and co-workers proposed a pathway with a 1,3-alternate intermediate for inversion of the cone conformer.[44, 45] Isomer NaC4A-I has a highly distorted cone form; one pair of benzene rings has a large angle (123˚, see Figures 6a and 10a). Hence, isomers NaC4A-IV and NaC4A-V (Figures 10b and 10c) seem to be formed easily from NaC4A-I by turning one or two phenol part(s) by smaller angles, through the oxygen-through-the-annulus rotation.[6] We

examine isomerization processes characteristics of C4A and Na^+•C4A by calculating the structure and the energy at transition states along isomerization coordinates. Figure 11 displays the energy of stable and transition-state conformations for (a) C4A and (b) Na^+•C4A calculated at the M05-2X/6-31+G(d) level of theory. All the transition-state structures are shown in the Electronic Supplementary Information. A transition state on direct pathways could not be found from cone to 1,3-alternate or to 1,2-alternate. This result suggests that the 1,3-alternate and 1,2-alternate conformers can be formed with stepwise manners from the cone isomer: (cone → partial-cone → 1,3-alternate) and (cone → partial-cone → 1,2-alternate). For bare C4A (Figure 11a), the energies of the transition states (TS1, TS2, and TS3) relative to that of the cone conformer are less than 75 kJ/mol. Hence, isomerization among the four conformers can probably occur at room temperature.[46] However, since the cone conformer is much more stable than the other three conformers by more than 20 kJ/mol, the cone structure is thermodynamically a dominant form for C4A. The energy of the transition state between the partial-cone and 1,3-alternate forms (TS2, 73.6 kJ/mol) is substantially higher than that between the partial-cone and 1,2-alternate form (TS3, 45.7 kJ/mol), thus it is plausible that the conformational inversion of the cone-shaped C4A occurs mainly through the 1,2-alternate form: (cone → partial-cone → 1,2-alternate → partial-cone → cone). In the case of the Na^+•C4A complex, the relative energies of all the transition states are slightly higher than those of bare C4A (Figure 11b). Hence, the partial-cone (NaC4A-IV) and 1,3-alternate (NaC4A-V) forms of Na^+•C4A are stabilized also kinetically with higher barriers, but these forms are still accessible from the cone one at room temperature, before the Na^+•C4A complex enters the cold ion trap in our experimental setup. A similar ion-dependent change of conformation was previously found for the synthesis of C4A derivatives in solution. Shinkai and

co-workers examined metal ion template effects on the conformer distribution in the synthesis of tetra-O-alkyl-C4As and tetrakis((ethoxycarbonyl)methoxy)-C4As systematically.[7,8] They changed alkali or alkaline earth metal ions in the base used for the synthesis, and analyzed the conformer distribution of products by ^{1}H NMR spectroscopy. These studies indicated that the conformer distribution can be controlled by metal ions used in the reactions, suggesting that the conformation of C4A derivatives is strongly dependent on metal ions attached to them.[7,8]

For conformational inversion of the cone-shaped Na^+•C4A complex to occur, the Na^+ ion should move to the opposite side of the C4A component. One plausible route of Na^+ ion exchange is "metal-tunneling" through a tube formed with four oxygen atoms and four benzene rings of the 1,3-alternate form, as proposed by Ikeda and Shinkai; here it has to be noted that the word "tunneling" in their paper does not have a quantum-mechanical meaning but just describes phenomena for metal ions to travel in the tube.[5] They reported that some C4A complexes with Ag^+, K^+, and Na^+ ions have a 1,3-alternate form and show "metal-tunneling" between two binding sites.[5] We examine the energetics of the metal exchange in the 1,3-alternate conformers of the Na^+•C4A and K^+•C4A complexes theoretically. Figure 12 shows the energy diagram of the metal exchange between the two biding sites in the 1,3-alternate forms (MC4A-V) of the (a) Na^+•C4A and (b) K^+•C4A complexes calculated at the M05-2X/6-31+G(d) level of theory. The vertical axis of Figure 12 is the energy relative to that of the cone conformers (MC4A-I). The structures of transition-state and stable forms along the metal exchange reaction are shown in Figure 13. The metal exchange process is quite different between the Na^+ and K^+ complexes. In the case of the Na^+•C4A complex, the conformer that has the Na^+ ion at the middle position of the 1,3-alternate is not a transition-state but a stable form. The structure of this isomer

(NaC4A-VII) is shown in Figure 13c. The Na^+ ion is surrounded by the four oxygen atoms and trapped in this pocket. As seen in Figure 12a, there is a high potential barrier (54.8 kJ/mol) between the 1,3-alternate form (NaC4A-V) and NaC4A-VII; the transition-state structure (TS4) is displayed in Figure 13b. As the Na^+ ion moves from one binding site to the other in the 1,3-alternate form (from left to right in Figure 13a), two phenol parts follow the Na^+ ion by rotating themselves, and the complex opens the conformation largely, because the electrostatic interaction between the Na^+ ion and the oxygen atoms is quite strong. In this process, the complex reduces its symmetry from C_2 to C_1, indicating that the rotation of the two phenol groups occurs one by one. Then the complex reaches to the transition state (TS4, Figure 13b) and to the stable form (NaC4A-VII, Figure 13c). Considering the energy of TS4 relative to that of the cone form (NaC4A-I) (77.1 kJ/mol, see Figure 12a), the intramolecular Na^+ exchange can occur at room temperature. Since the intermediate (NaC4A-VII, 45.6 kJ/mol) is not so stable compared to the partial-cone (NaC4A-IV, 11.2 kJ/mol) and 1,3-alternate (NaC4A-V, 22.3 kJ/mol) forms, NaC4A-VII would not contribute highly to the UVPD spectrum of Na^+•C4A. For the K^+•C4A complex, the K^+ ion is too large to be encapsulated at the center of the 1,3-alternate form, giving a transition-state structure (TS4, Figure 13d). The energy of TS4 (97.9 kJ/mol, see Figure 12b) is higher than that of Na^+•C4A; the K^+ exchange is not likely to occur in the K^+•C4A even at room temperature.

4. Summary

We have measured UV photodissociation (UVPD) spectra of calix[4]arene (C4A) complexes with alkali metal ions, M^+•C4A (M = Na, K, Rb, and Cs), in the

34000–37000 cm^{-1} region, under cold (~10 K) conditions in the gas phase by using an electrospray ion source and a cold quadrupole ion trap (QIT). The Na^+•C4A and K^+•C4A complexes exhibit several sharp vibronic bands, while the UVPD spectra of the Rb^+ and Cs^+ complexes show only broad features in this region. Most of the features in the UVPD spectra of the M^+•C4A complexes can be attributed to the most stable, cone isomers, MC4A-I. In isomers MC4A-I, the M^+ ion is included inside the cavity of C4A; the structure is largely distorted with C_2 symmetry from a C_4 form of bare C4A. In the Na^+ and K^+ complexes, a pair of two benzene rings faces to each other with a short distance (< 6 Å), which results in effective overlap of π clouds of the two benzene rings and an electronic transition localized on this pair. Only this localized electronic transition (S_2–S_0) of the Na^+ and K^+ complexes shows sharp band features in the UVPD spectra. For the Na^+•C4A complex, the UVPD result suggests the coexistence of the other isomers (NaC4A-IV and NaC4A-V) under our experimental condition. Isomers NaC4A-IV and NaC4A-V have a partial-cone and 1,3-alternate conformation on the C4A part, respectively, and show a very broad feature in the UVPD spectrum. This broad feature of the absorption may probably represent a fast dynamics due to a floppy nature of Na^+ encapsulation in the electronic excited states. The energetics of the isomerization reactions of Na^+•C4A suggests that the coexistence of the partial-cone and 1,3-alternate conformers is ascribed to higher stability of these forms, both kinetically and thermodynamically, compared to corresponding isomers of C4A and the other M^+•C4A complexes.

Acknowledgment

The authors wish to acknowledge Prof. Osamu Takahashi, Hiroshima University, for his valuable advice for the transition-state calculations. The quantum chemical calculations in this study were performed partly using Research Center for Computational Science, Okazaki, Japan. This work was supported by JSPS KAKENHI Grant Number 16H04098.

Electronic Supplementary Information: The structures of the M^+•C4A (M = Na, K, Rb, and Cs) complexes obtained in the quantum chemical calculations.

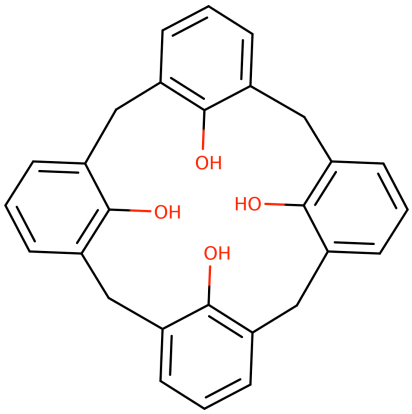

Scheme 1.

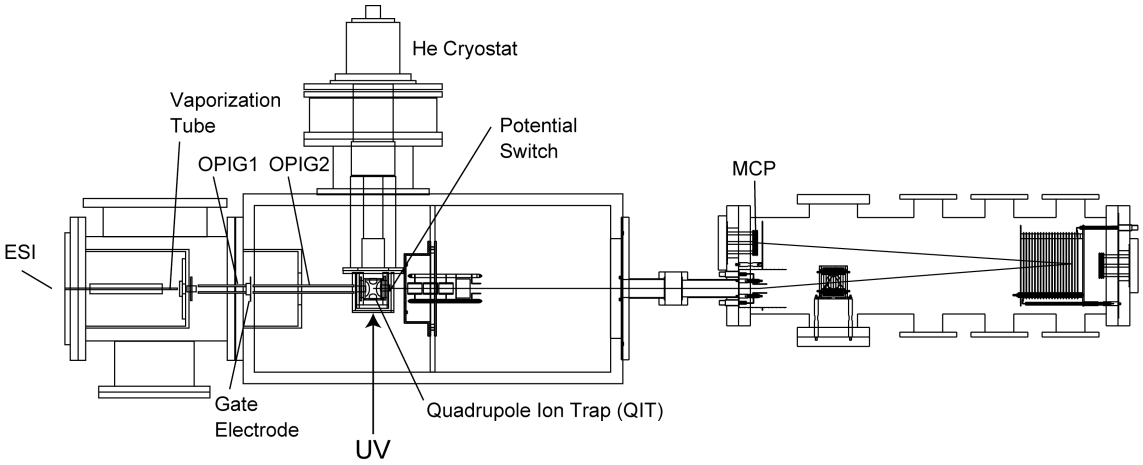

Figure 1. Schematic drawing of a mass spectrometer for UVPD spectroscopy under cold conditions in the gas phase.

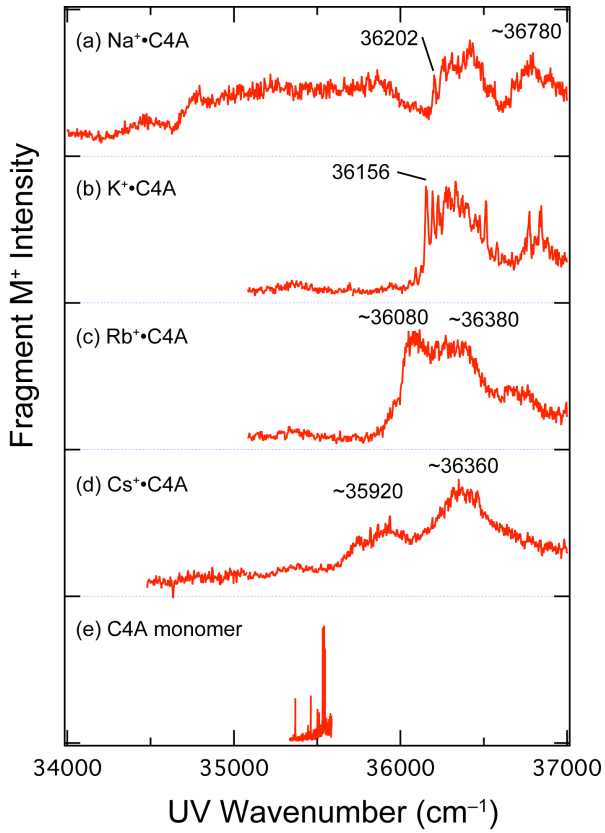

Figure 2. (a–d) UVPD spectra of the M^+•C4A (M = Na, K, Rb, and Cs) complexes. (e) Electronic spectrum of jet-cooled C4A (Ref. 21).

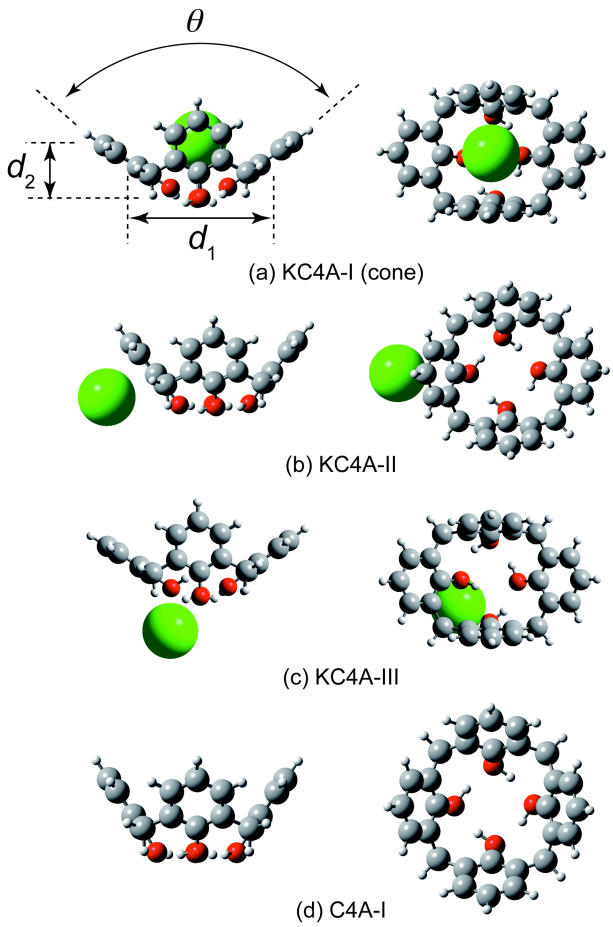

Figure 3. Stable structures of the K^+•C4A complexes and bare C4A with a cone form.

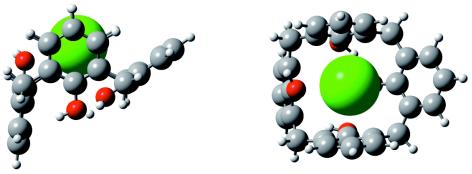

(a) KC4A-IV (partial-cone)

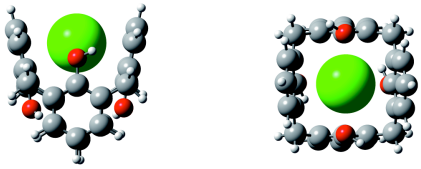

(b) KC4A-V (1,3-alternate)

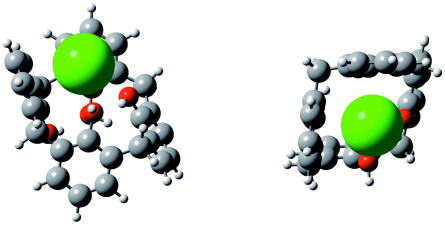

(c) KC4A-VI (1,2-alternate)

Figure 4. Stable structures of the K^+•C4A complexes with conformations other than a cone form.

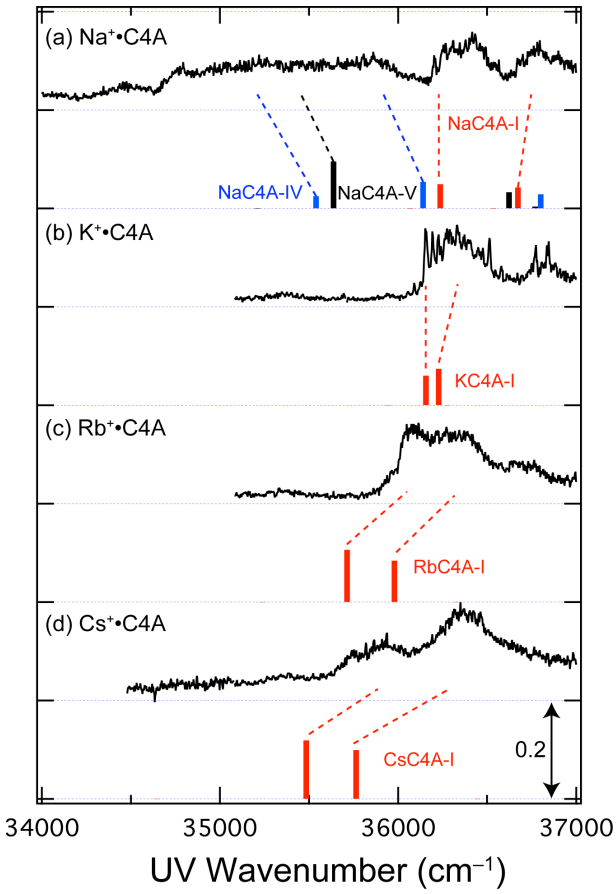

Figure 5. Calculated oscillator strengths of the M^+•C4A (M = Na, K, Rb, and Cs) complexes (red, blue, and black bars) with the UVPD spectra (black curves). The TD-DFT calculations are performed at the M05-2X/6-31+G(d) level of theory. A scaling factor of 0.8426 is employed for calculated transition energies. This factor is determined so as to reproduce the position of the sharp UVPD band of the K^+•C4A complex at 36156 cm^{-1} with the S_2–S_0 transition energy of isomer KC4A-I.

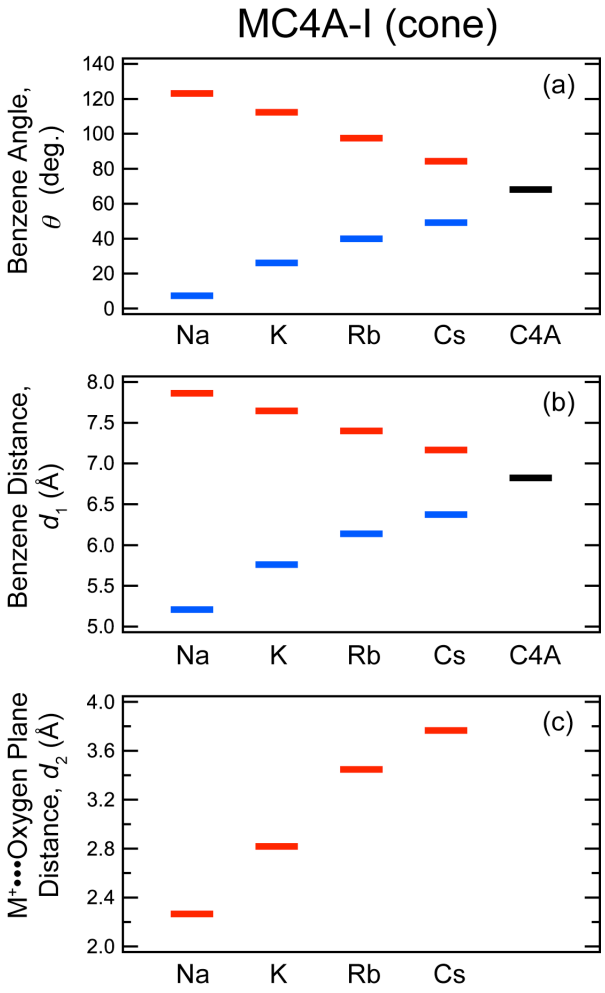

Figure 6. Geometric parameters of isomers MC4A-I (cone isomers) for the M^+•C4A (M = Na, K, Rb, and Cs) complexes with those of C4A (C4A-I). The definition of θ, d_1, and d_2 is illustrated in Figure 3a. For θ and d_1, there are two values for each isomer, because there are two pairs of benzene rings facing to each other.

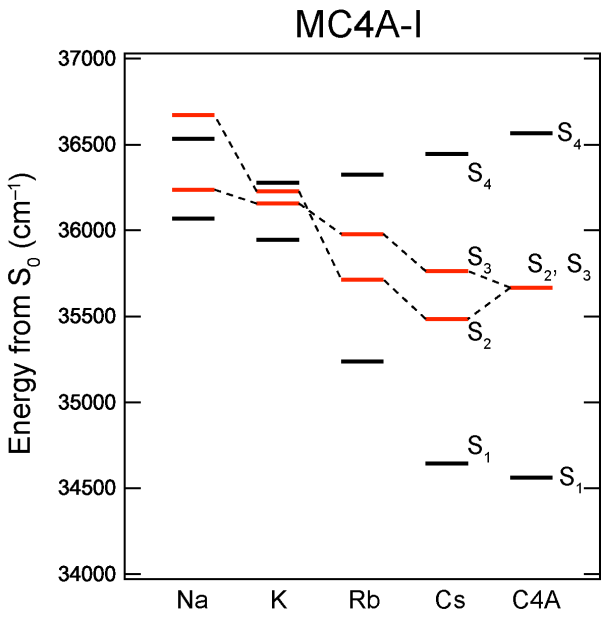

Figure 7. Energy levels of electronic excited states for isomers MC4A-I (M = Na, K, Rb, and Cs) calculated at the M05-2X/6-31+G(d) level of theory. A scaling factor of 0.8426 is employed for the calculated energy. The energy levels of bare C4A (C4A-I, see Figure 3d) are also shown. The red lines present the energy levels that are strongly dipole-allowed from the S_0 state.

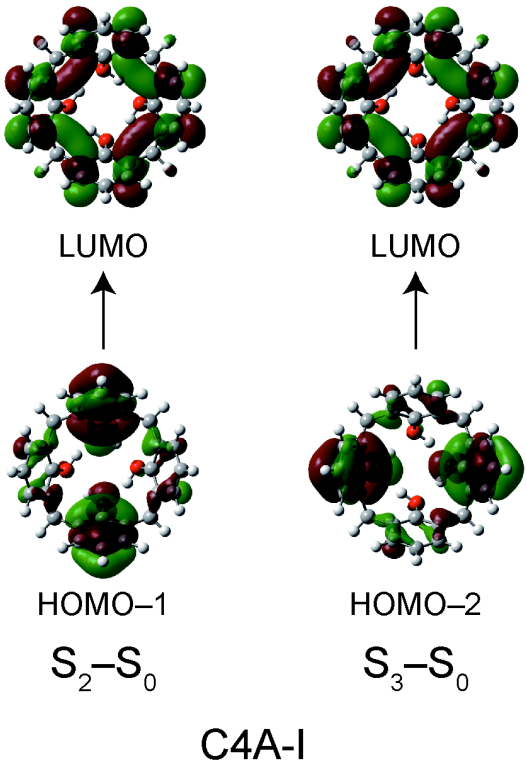

Figure 8. MOs relevant to electronic transitions of C4A-I.

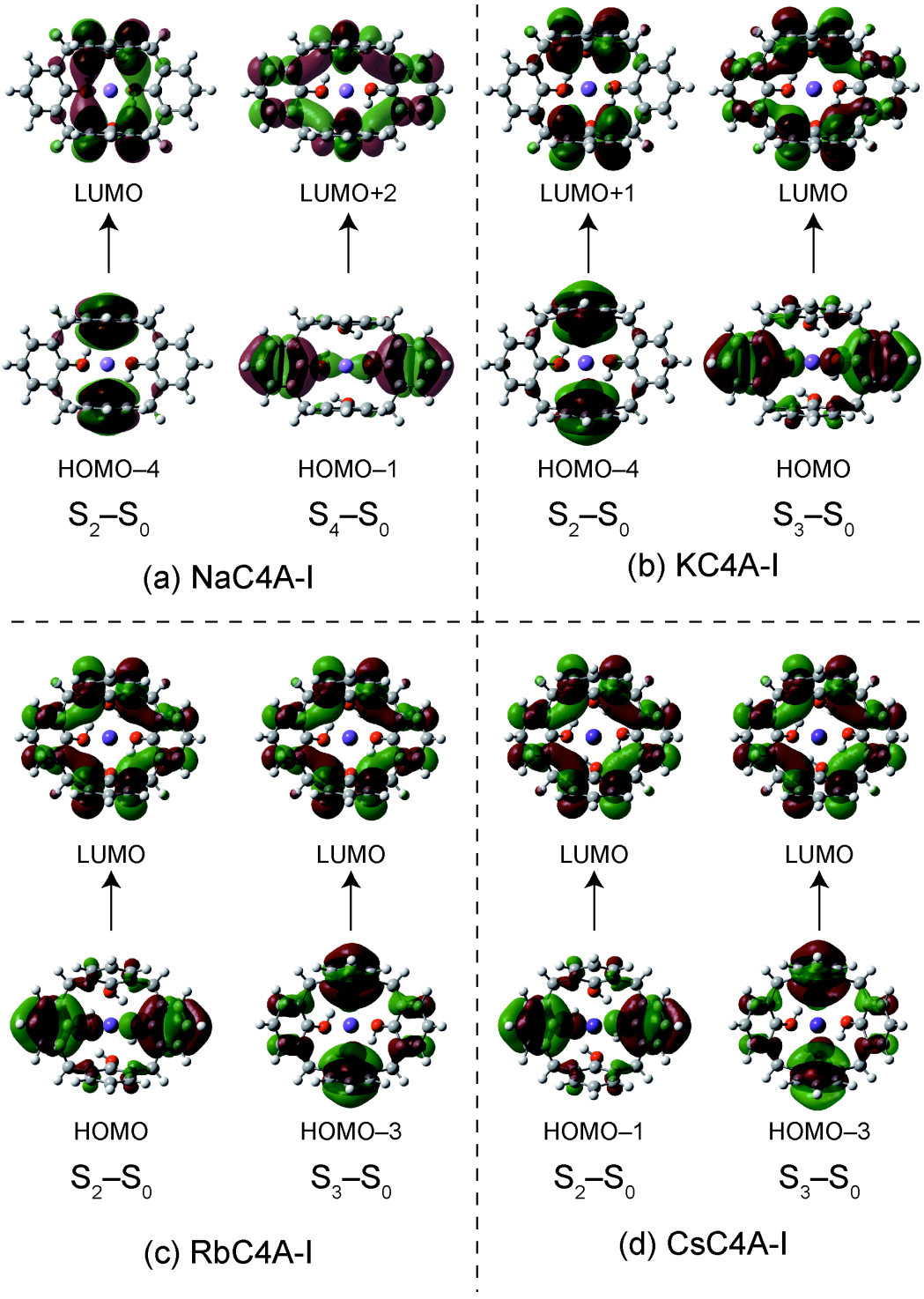

Figure 9. MOs relevant to electronic transitions of isomers MC4A-I (M = Na, K, Rb, and Cs).

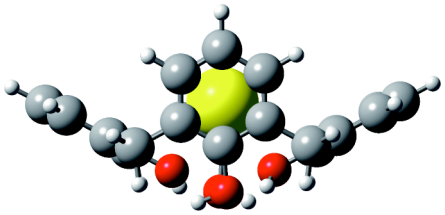

(a) NaC4A-I (cone)

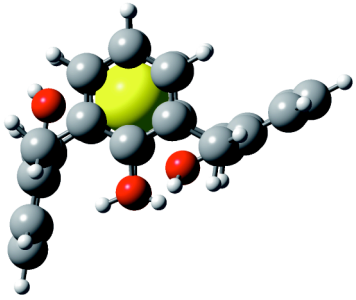

(b) NaC4A-IV (partial-cone)

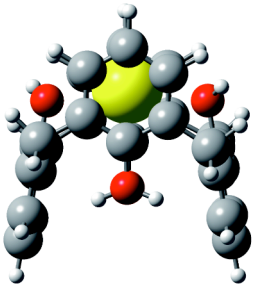

(c) NaC4A-V (1,3-alternate)

Figure 10. Stable structures of the Na^{+}•C4A complex.

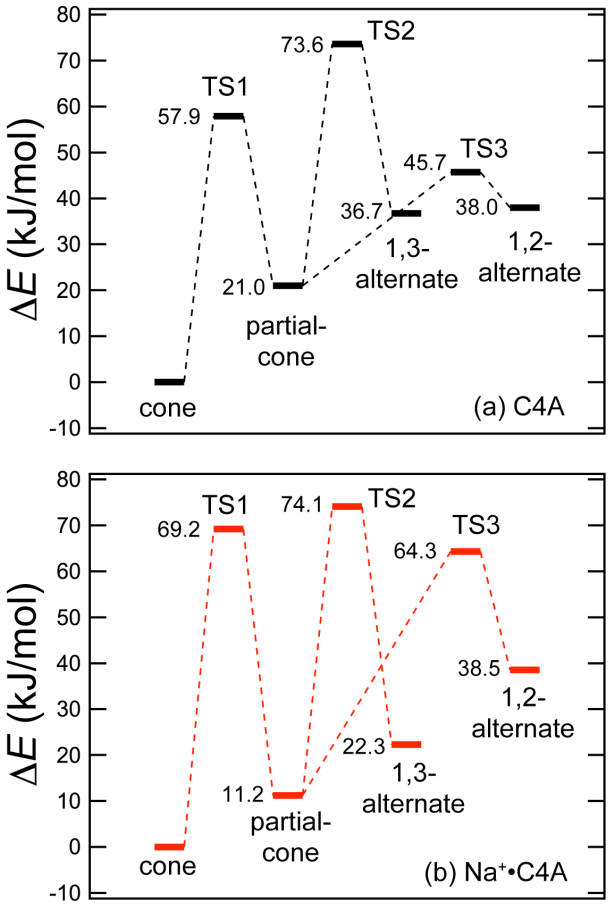

Figure 11. Energy levels of stable and transition-state conformations of (a) C4A and (b) Na^+•C4A complex calculated at the M05-2X/6-31+G(d) level of theory. These energy levels are corrected by zero-point energy.

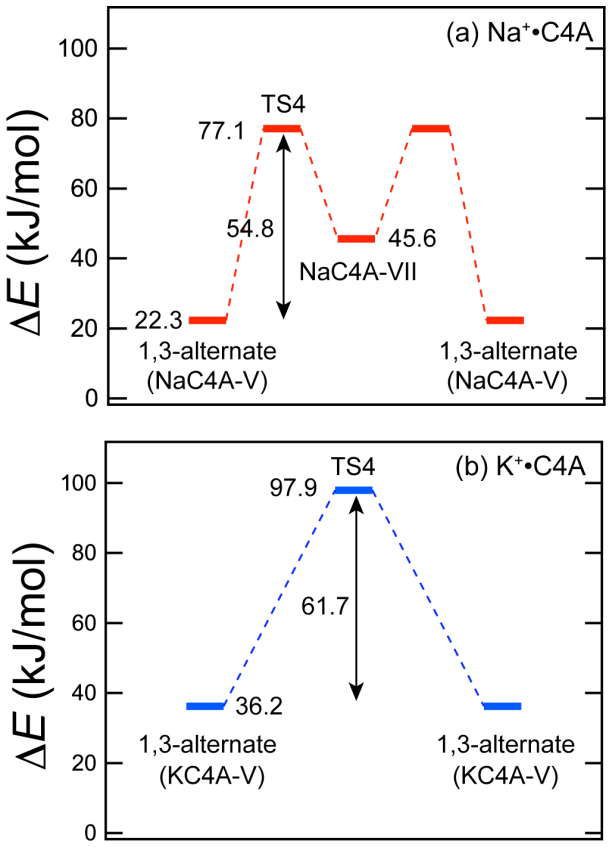

Figure 12. Energy levels along the metal exchange reaction in the 1,3-alternate conformers of (a) Na^+•C4A and (b) K^+•C4A calculated at the M05-2X/6-31+G(d) level of theory. The vertical axis is the energy relative to that of the cone conformers (MC4A-I). These energy levels are corrected by zero-point vibrational energy.

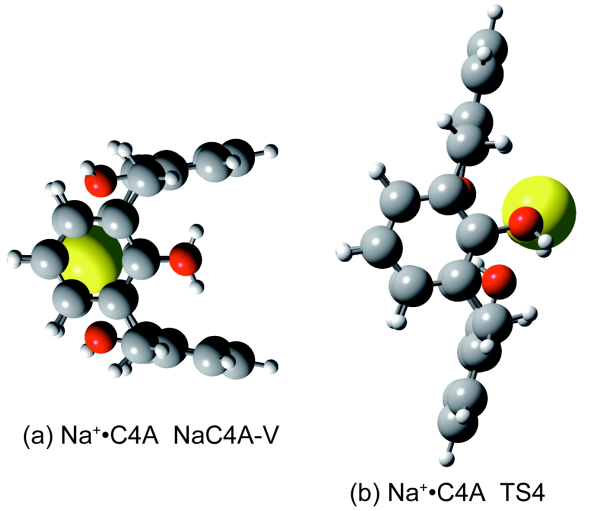

Figure 13. Transition-state and stable conformations along the metal exchange reaction in the 1,3-alternate conformers (see Figure 12).

Table 1. Relative total energies (kJ/mol) of stable isomers for the M^+•C4A (M = Na, K, Rb, and Cs) complexes and bare C4A calculated at the M05-2X/6-31+G(d) level of theory. These values are corrected by the zero point energy.

M	MC4A-I (cone)	MC4A-II	MC4A-III	MC4A-IV (partial-cone)	MC4A-V (1,3-alternate)	MC4A-VI (1,2-alternate)
Na	0	102.1	96.5	11.2	22.3	38.5
K	0	92.9	100.9	16.7	36.2	62.7
Rb	0	66.6	72.8	22.8	49.7	61.7
Cs	0	62.6	65.0	25.1	57.9	63.5
(C4A)	0	–	–	21.0	36.7	38.0

Table 2. Transition energies (eV) and oscillator strengths (in parentheses) for isomers MC4A-I and C4A-I calculated at the M05-2X/6-31+G(d) level of theory. A scaling factor of 0.8426 is employed for the calculated energies.

transitions	NaC4A-I	KC4A-I	RbC4A-I	CsC4A-I	C4A-I
S_1–S_0	4.472 (0.0000)	4.457 (0.0000)	4.369 (0.0000)	4.295 (0.0001)	4.285 (0.0001)
S_2–S_0	4.493 (0.0494)	4.483 (0.0600)	4.428 (0.1061)	4.399 (0.1187)	4.422 (0.1112)
S_3–S_0	4.530 (0.0000)	4.492 (0.0738)	4.461 (0.0839)	4.434 (0.0992)	4.422 (0.1112)
S_4–S_0	4.547 (0.0425)	4.498 (0.0000)	4.504 (0.0000)	4.519 (0.0000)	4.534 (0.0000)

Table of Contents:

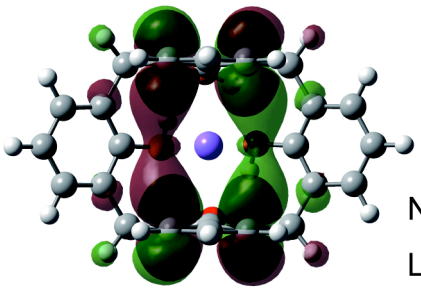

Na^+•C4A

LUMO

UV spectra of M^+•(calix[4]arene) complexes under cold gas-phase conditions suggest the interaction between two of the four benzene rings in the M = Na and K complexes.

References

1. C. D. Gutsche and R. Muthukrishnan, *J. Org. Chem.*, 1978, **43**, 4905-4906.
2. C. D. Gutsche and J. A. Levine, *J. Am. Chem. Soc.*, 1982, **104**, 2652-2653.
3. C. D. Gutsche, *Acc. Chem. Res.*, 1983, **16**, 161-170.
4. S. Shinkai, *Tetrahedron*, 1993, **49**, 8933-8968.
5. A. Ikeda and S. Shinkai, *J. Am. Chem. Soc.*, 1994, **116**, 3102-3110.
6. A. Ikeda and S. Shinkai, *Chem. Rev.*, 1997, **97**, 1713-1734.
7. K. Iwamoto, K. Araki and S. Shinkai, *J. Org. Chem.*, 1991, **56**, 4955-4962.
8. K. Iwamoto and S. Shinkai, *J. Org. Chem.*, 1992, **57**, 7066-7073.
9. T. Haino, M. Yanase and Y. Fukazawa, *Angew. Chem. Int. Ed.*, 1997, **36**, 259-260.
10. T. Haino, M. Yanase and Y. Fukazawa, *Tetrahedron Lett.*, 1997, **38**, 3739-3742.
11. T. Haino, M. Yanase and Y. Fukazawa, *Angew. Chem. Int. Ed.*, 1998, **37**, 997-998.
12. R. M. Izatt, J. D. Lamb, R. T. Hawkins, P. R. Brown, S. R. Izatt and J. J. Christensen, *J. Am. Chem. Soc.*, 1983, **105**, 1782-1785.
13. S. R. Izatt, R. T. Hawkins, J. J. Christensen and R. M. Izatt, *J. Am. Chem. Soc.*, 1985, **107**, 63-66.
14. C. D. Gutsche and L. J. Bauer, *J. Am. Chem. Soc.*, 1985, **107**, 6052-6059.
15. C. D. Gutsche, B. Dhawan, J. A. Levine, K. Hyun No and L. J. Bauer, *Tetrahedron*, 1983, **39**, 409-426.
16. G. D. Andreetti, R. Ungaro and A. Pochini, *J. Chem. Soc., Chem. Commun.*, 1979, 1005-1007.
17. G. D. Andreetti, A. Pochini and R. Ungaro, *J. Chem. Soc. Perkin Trans. 2*, 1983, 1773-1779.
18. F. Benevelli, W. Kolodziejski, K. Wozniak and J. Klinowski, *Chem. Phys. Lett.*, 1999, **308**, 65-70.
19. R. J. Bernardino and B. J. C. Cabral, *J. Phys. Chem. A*, 1999, **103**, 9080-9085.
20. F. Huang, J. Yang, A. Hao, X. Wu, R. Liu and Q. Ma, *Spectrochim. Acta A: Mol. Biomol. Spectrosc.*, 2001, **57**, 1025-1030.
21. T. Ebata, Y. Hodono, T. Ito and Y. Inokuchi, *J. Chem. Phys.*, 2007, **126**, 141101.
22. T. Ebata, N. Hontama, Y. Inokuchi, T. Haino, E. Apra and S. S. Xantheas, *Phys. Chem. Chem. Phys.*, 2010, **12**, 4569-4579.
23. N. Hontama, Y. Inokuchi, T. Ebata, C. Dedonder-Lardeux, C. Jouvet and S. S. Xantheas, *J. Phys. Chem. A*, 2010, **114**, 2967-2972.
24. S. Kaneko, Y. Inokuchi, T. Ebata, E. Apra and S. S. Xantheas, *J. Phys. Chem. A*, 2011, **115**, 10846-10853.
25. O. V. Boyarkin, S. R. Mercier, A. Kamariotis and T. R. Rizzo, *J. Am. Chem. Soc.*, 2006, **128**, 2816-2817.
26. A. Svendsen, U. J. Lorenz, O. V. Boyarkin and T. R. Rizzo, *Rev. Sci. Instrum.*, 2010, **81**, 073107.
27. C. M. Choi, J. H. Lee, Y. H. Choi, H. J. Kim, N. J. Kim and J. Heo, *J. Phys. Chem. A*, 2010, **114**, 11167-11174.
28. Y. Inokuchi, O. V. Boyarkin, R. Kusaka, T. Haino, T. Ebata and T. R. Rizzo, *J. Am. Chem. Soc.*, 2011, **133**, 12256-12263.

29. Y. Inokuchi, O. V. Boyarkin, R. Kusaka, T. Haino, T. Ebata and T. R. Rizzo, *J. Phys. Chem. A*, 2012, **116**, 4057-4068.
30. Y. Inokuchi, R. Kusaka, T. Ebata, O. V. Boyarkin and T. R. Rizzo, *ChemPhysChem*, 2013, **14**, 649-660.
31. Y. Inokuchi, T. Ebata, T. R. Rizzo and O. V. Boyarkin, *J. Am. Chem. Soc.*, 2014, **136**, 1815-1824.
32. Y. Inokuchi, T. Ebata and T. R. Rizzo, *J. Phys. Chem. A*, 2015, **119**, 8097-8105.
33. Y. Inokuchi, T. Ebata and T. R. Rizzo, *J. Phys. Chem. A*, 2015, **119**, 11113-11118.
34. Y. Inokuchi, T. Haino, R. Sekiya, F. Morishima, C. Dedonder, G. Feraud, C. Jouvet and T. Ebata, *Phys. Chem. Chem. Phys.*, 2015, **17**, 25925-25934.
35. Y. Inokuchi, M. Nakatsuma, M. Kida and T. Ebata, *J. Phys. Chem. A*, 2016, **120**, 6394-6401.
36. Y. Inokuchi, M. Kida and T. Ebata, *J. Phys. Chem. A*, 2017, **121**, 954-962.
37. Y. Inokuchi, K. Soga, K. Hirai, M. Kida, F. Morishima and T. Ebata, *J. Phys. Chem. A*, 2015, **119**, 8512-8518.
38. H. Kang, G. Féraud, C. Dedonder-Lardeux and C. Jouvet, *J. Phys. Chem. Lett.*, 2014, **5**, 2760-2764.
39. Y. Kobayashi, Y. Inokuchi and T. Ebata, *J. Chem. Phys.*, 2008, **128**, 164319.
40. M. J. Frisch, G. W. Trucks, H. B. Schlegel, G. E. Scuseria, M. A. Robb, J. R. Cheeseman, G. Scalmani, V. Barone, B. Mennucci, G. A. Petersson, H. Nakatsuji, M. Caricato, X. Li, H. P. Hratchian, A. F. Izmaylov, J. Bloino, G. Zheng, J. L. Sonnenberg, M. Hada, M. Ehara, K. Toyota, R. Fukuda, J. Hasegawa, M. Ishida, T. Nakajima, Y. Honda, O. Kitao, H. Nakai, T. Vreven, J. Montgomery, J. A., J. E. Peralta, F. Ogliaro, M. Bearpark, J. J. Heyd, E. Brothers, K. N. Kudin, V. N. Staroverov, R. Kobayashi, J. Normand, K. Raghavachari, A. Rendell, J. C. Burant, S. S. Iyengar, J. Tomasi, M. Cossi, N. Rega, N. J. Millam, M. Klene, J. E. Knox, J. B. Cross, V. Bakken, C. Adamo, J. Jaramillo, R. Gomperts, R. E. Stratmann, O. Yazyev, A. J. Austin, R. Cammi, C. Pomelli, J. W. Ochterski, R. L. Martin, K. Morokuma, V. G. Zakrzewski, G. A. Voth, P. Salvador, J. J. Dannenberg, S. Dapprich, A. D. Daniels, Ö. Farkas, J. B. Foresman, J. V. Ortiz, J. Cioslowski and D. J. Fox, *Journal*, 2009.
41. Y. Zhao, N. E. Schultz and D. G. Truhlar, *J. Chem. Theory Comput.*, 2006, **2**, 364-382.
42. K. L. Schuchardt, B. T. Didier, T. Elsethagen, L. S. Sun, V. Gurumoorthi, J. Chase, J. Li and T. L. Windus, *J. Chem. Inf. Model.*, 2007, **47**, 1045-1052.
43. D. Feller, *J. Comput. Chem.*, 1996, **17**, 1571-1586.
44. H. Kämmerer, G. Happel and F. Caesar, *Makromol. Chem.*, 1972, **162**, 179-197.
45. G. Happel, B. Mathiasch and H. Kämmerer, *Makromol. Chem.*, 1975, **176**, 3317-3334.
46. J. McMurry, *Organic Chemistry*, Brooks/Cole Publishing Company, California, 5th ed. edn., 2000.